Molecular Biology of the Cell
Vol. 19, 3823–3835, September 2008

The DHR1 Domain of DOCK180 Binds to SNX5 and Regulates Cation-independent Mannose 6-phosphate Receptor Transport

Shigeo Hara,*† Etsuko Kiyokawa,‡ Shun-ichiro Iemura,§ Tohru Natsume,§ Thomas Wassmer,‖ Peter J. Cullen,‖ Hiroshi Hiai,¶ and Michiyuki Matsuda*†‡

*Department of Pathology and Biology of Diseases, Graduate School of Medicine, Kyoto University, Kyoto 606-8501, Japan; †Department of Signal Transduction, Research Institute for Microbial Diseases, Osaka University, Suita, Osaka 565-0871, Japan; ‡Laboratory of Bioimaging and Cell Signaling, Graduate School of Biostudies, Kyoto University, Kyoto 606-8501, Japan; §National Institute of Advanced Industrial Science and Technology, Biological Information Research Center, Tokyo 135-0064, Japan; ‖Henry Wellcome Integrated Signalling Laboratories, Department of Biochemistry, School of Medical Sciences, University of Bristol, Bristol BS8 1TD, United Kingdom; and ¶Shiga Medical Center Research Institute, Moriyama, Shiga 524-8524, Japan

Submitted March 26, 2008; Revised June 3, 2008; Accepted June 25, 2008
Monitoring Editor: Adam Linstedt

DOCK180 is the archetype of the DOCK180-family guanine nucleotide exchange factor for small GTPases Rac1 and Cdc42. DOCK180-family proteins share two conserved domains, called DOCK homology region (DHR)-1 and -2. Although the function of DHR2 is to activate Rac1, DHR1 is required for binding to phosphoinositides. To better understand the function of DHR1, we searched for its binding partners by direct nanoflow liquid chromatography/tandem mass spectrometry, and we identified sorting nexins (SNX) 1, 2, 5, and 6, which make up a multimeric protein complex mediating endosome-to-*trans*-Golgi-network (TGN) retrograde transport of the cation-independent mannose 6-phosphate receptor (CI-MPR). Among these SNX proteins, SNX5 was coimmunoprecipitated with DOCK180 most efficiently. In agreement with this observation, DOCK180 colocalized with SNX5 at endosomes. The RNA interference-mediated knockdowns of SNX5 and DOCK180, but not Rac1, resulted in the redistribution of CI-MPR from TGN to endosomes. Furthermore, expression of the DOCK180 DHR1 domain was sufficient to restore the perturbed CI-MPR distribution in DOCK180 knockdown cells. These data suggest that DOCK180 regulates CI-MPR trafficking via SNX5 and that this function is independent of its guanine nucleotide exchange factor activity toward Rac1.

INTRODUCTION

DOCK180 was originally identified as one of two major binding proteins of the adaptor protein CRK and became the archetype of the DOCK180-family guanine nucleotide exchange factor (GEF) for Rac1 and Cdc42 (Hasegawa *et al.*, 1996; Cote and Vuori, 2002; Meller *et al.*, 2002). Genetic studies have identified orthologues of DOCK180 in *Caenorhabditis elegans* (CED-5) and *Drosophila melanogaster* (Myoblast city, MBC), respectively, which make up an evolutionarily conserved protein group called the CDM (CED-5, *D*OCK180, *M*BC)-family (Wu and Horvitz, 1998). The crucial role of these DOCK180-family proteins has been demonstrated in various biological processes. In *C. elegans*, CED-5 acts in the engulfment of apoptotic cell corpses and in the migration of gonadal distal tip cells (Wu and Horvitz, 1998). MBC is necessary for myoblast fusion and dorsal closure during the embryogenesis of *D. melanogaster* (Erickson *et al.*, 1997). Plasma membrane-targeted mammalian DOCK180 alters the morphology of COS cells from spindled to flat and polygonal shape, and coexpression of DOCK180 with both CRKII and $p130^{Cas}$ induces the accumulation of these proteins at the focal adhesions in NIH3T3 cells (Hasegawa *et al.*, 1996; Kiyokawa *et al.*, 1998b).

DOCK180 contains N-terminal SH3 and C-terminal proline-rich domains, which function as docking sites for ELMO (Gumienny *et al.*, 2001) and CRKII (Hasegawa *et al.*, 1996), respectively. Both ELMO and CRKII function to mediate extracellular signals via RhoG (Katoh and Negishi, 2003) and $p130^{Cas}$ (Kiyokawa *et al.*, 1998a), respectively, and to enhance DOCK180-induced Rac1 activation. In addition to the SH3 and proline-rich domains, subsequent studies identified two other regions, designated DHR1 and DHR2 (or CZH1 and CZH2/DOCKER, respectively) (Cote and Vuori, 2002; Meller *et al.*, 2002), both of which showed high sequence homology among the 11 human DOCK180 superfamily proteins. A succession of evidence has demonstrated that DHR2 functions as a guanine nucleotide exchange factor for Rho-family proteins (Fukui *et al.*, 2001; Cote and Vuori, 2002; Meller *et al.*, 2002; Watabe-Uchida *et al.*, 2006). It

This article was published online ahead of print in *MBC in Press* (http://www.molbiolcell.org/cgi/doi/10.1091/mbc.E08–03–0314) on July 2, 2008.

Address correspondence to: Etsuko Kiyokawa (kiyokawa@lif.kyoto-u.ac.jp).

Abbreviations used: BAR, Bin/amphiphysin/Rvs; DHR, DOCK homology region; MPR, mannose 6-phosphate receptor; PBS, phosphate-buffered saline; $PI(3,5)P_2$, phosphatidylinositol 3,5-bisphosphate; PIP_3, phosphatidylinositol 3,4,5-trisphosphate; PX, phox homology; RLC, rupture of a lens cataract; SNX, sorting nexin; TGN, *trans*-Golgi network; Vps, vacuolar protein sorting.

has been shown that a DOCK180 mutant without DHR1 fails to promote cell migration, irrespective of its intact activity toward Rac GTP loading (Cote *et al.*, 2005). In vitro data indicated that phosphatidylinositol 3,5-bisphosphate [$PI(3,5)P_2$] and phosphatidylinositol 3,4,5-trisphosphate (PIP_3) bind to DHR1 and that PIP_3 recruits DOCK180 through DHR1 at the site of lamellipodia induced by platelet-derived growth factor (Cote *et al.*, 2005).

Sorting nexins (SNXs) are cytoplasmic and membrane-associated proteins that share a phox homology (PX)-domain, which recognizes various phosphoinositides (Teasdale *et al.*, 2001). SNX1 was first identified as a binding protein to epidermal growth factor receptor (EGFR) by yeast two-hybrid screening, and it was found to enhance receptor degradation when overexpressed (Kurten *et al.*, 1996). A comparison of amino acid sequences revealed that SNX1 is an ortholog of a yeast protein called Vacuolar protein sorting 5p (Vps5p) (Horazdovsky *et al.*, 1997). Vps5p is a constituent of the heteropentameric complex called retromer, which consists of Vps35p, Vps29p, Vps26p, Vps5p, and Vps17p, and regulates the endosome-to-Golgi transport of proteins (Seaman *et al.*, 1998). In yeast, newly synthesized acidic hydrolases are sorted to vacuoles by hydrolase receptor Vps10p (Seaman, 2005). After the delivery of hydrolase, Vps10p is recycled back to the late Golgi apparatus. In mammalian cells, the delivery of hydrolases from *trans*-Golgi network (TGN) to lysosome is mediated by the mannose 6-phosphate receptors (MPRs) (Kornfeld and Mellman, 1989). There are two distinct MPRs in mammalian cells: the 46-kDa cation-dependent MPR (CD-MPR) and the 300-kDa cation-independent MPR (CI-MPR). Neither MPR shares any significant sequence homology with Vps10p but, like Vps10p, both have an essentially identical function and cycle between the TGN and the endosome (Seaman, 2005). The small interfering RNA (siRNA)-mediated knockdown technique has shown that suppression of VPS26 and SNX1 induces CI-MPR mislocalization to the peripheral vesicular structure from TGN (Carlton *et al.*, 2004; Seaman, 2004). Recently, a siRNA-mediated loss-of-function screen for 30 SNX members identified SNX5 and SNX6 as functional counterparts of Vps17p (Wassmer *et al.*, 2007).

Here, we identify SNX5 as a binding partner of DHR1 of DOCK180. Furthermore, we show a potential role of DOCK180 in retromer-mediated retrograde transport of CI-MPR, which is independent of the previously reported binding partners such as ELMO, CRK, and Rac1.

MATERIALS AND METHODS

Expression Plasmids

The cDNA encoding the full-length or truncated SNXs were amplified by polymerase chain reaction (PCR) with primer sets containing XhoI or SalI sequences at 5′ terminus, and NotI at 3′ terminus, and subcloned into pDrive (QIAGEN, Hilden, Germany) or pCR2.1-TOPO vector (Invitrogen, Paisley, United Kingdom). As the template for PCR, the plasmids (Teasdale *et al.*, 2001; Cozier *et al.*, 2002; Carlton *et al.*, 2005) or cDNA from HeLa cells was used. After the nucleotide sequences were confirmed, the cDNAs were cloned to pCAGGS-EGFP, pCXN2-GST, pCXN2-mRFP, or pCA-FLAG, generating pCA-EGFP-SNX5, pCXN2-GST-SNX5, pCXN2-mRFP-SNX5, pCA-FLAG-SNX1, -SNX2, -SNX4, -SNX5, -SNX6b (denoted as SNX6), -SNX5-PX (amino acids 1-168), -SNX5-BAR (169-404), -SNX5-Helix1 (1-261), and -SNX5-Helix2 (1-343). Similarly, DHR1 domains of DOCK-family proteins are generated. The following cDNAs were used as templates: pCA-FLAG-DOCK180 for DOCK180 (Hasegawa *et al.*, 1996), pGFP-DOCK2 for DOCK2 (Nishihara *et al.*, 1999), pCXN2-mRFP-DOCK4 for DOCK4 (Yajnik *et al.*, 2003), and KIAA0299 for DOCK3, KIAA1395 for DOCK6, and KIAA1771 for DOCK9 (Kazusa DNA Research Institute, Chiba, Japan). Full-length DOCK180 was inserted into pCAGGS-EGFP and pCXN2-mVenus to generate pCA-EGFP-DOCK180 and pCXN2-mVenus-DOCK180, respectively. The plasmids pCA-FLAG-ERK2 was described previously (Fujioka *et al.*, 2006). pCA-FLAG-mSos1 is the expression plasmid for mouse Sos1 protein. To construct the rupture of a lens cataract (RLC) mutant of human DOCK180, the DHR1 domain carrying the RLC deletion mutant was first constructed. The RLC region, which corresponds to amino acids 488-496 of human DOCK180, was deleted by overlapping PCR. The first PCR reactions were performed independently with primer set #1, SalI-DHR1F-F (CACCGTCGACGGTGATGTTCGAAATGATATC) and RLC-del-DOCK1-R (GTCCTCGATGGGAATGGCCAGCTTTACTTGGTAGTAAATCAC) and #2, RLC-del-DOCK1-F (GTGATTTACTACCAAGTAAAGGTGGCCATTCCCATCG-AGGAC) and DHR1stop-R-NotI (GGGCGGCCGCTCACTCCATCATGATGTT-GAAGAG). The amplified DNA fragments were used as templates in the second PCR with primers SalI-DHR1F-F and DHR1stop-R-NotI. The nucleotide sequences of the second PCR product were confirmed after being cloned into pENTRY vector (Invitrogen). The RLC cDNA fragment was cloned into pEBG to generate pEBG-DHR1-RLC. After the full-length DOCK180-RLC was established in pBlueScript vector, expression vector pCXN2-mVenus-DOCK180-RLC was constructed. pSuper.retro.puro vector (Oligoengine, Seattle, WA) was used for short hairpin RNA (shRNA). The shRNA sequences targeting DOCK180 and firefly luciferase were 5′-GTTTCTTCAGGACACGTTG-3′ and 5′-GATTATGTCCGGT-TATGTA-3′, respectively. For RNA interference (RNAi), rescue experiments, an shRNA-resistant construct was created by introducing seven silent point mutations in the target sequences (TTCCTGCAGGATACCTTAGACGCT), generating pCA-EGFP-DOCK180^R, -DHR1^R, and -DHR1^R-RLC. For retroviral infection, a Moloney murine leukemia virus-based retroviral vector plasmid, pMSCVpac-EGFP-SNX5, was constructed.

Antibodies

The polyclonal antibodies against DOCK180 were developed in our laboratory and described previously (Hasegawa *et al.*, 1996). Antibodies used in this study were purchased as follows: Mouse anti-FLAG antibody (Sigma-Aldrich, St. Louis, MO), mouse anti-green fluorescent protein (GFP) antibody (Clontech, Mountain View, CA), mouse anti-pan extracellular signal-regulated kinase (ERK) antibody (BD Biosciences, San Jose, CA), mouse anti-SNX1 antibody (BD Biosciences), goat anti-SNX5 antibody (Santa Cruz Biotechnology, Santa Cruz, CA), rabbit anti-SOS2 antibody (Santa Cruz Biotechnology), sheep anti-TGN46 antibody (Serotec, Oxford, United Kingdom), mouse anti-Golgin97 antibody (Invitrogen), mouse monoclonal anti-CD8 antibody (Alexis Biochemicals, Lausen, Switzerland), mouse Alexa Fluor488-conjugated anti-CD8 antibody (Serotec), Alexa Fluor488-conjugated mouse monoclonal anti-CD8 antibody (Serotec), mouse anti-early endosomal antigen (EEA)1 antibody (BD Biosciences), mouse anti-tubulin antibody (Calbiochem, San Diego, CA), anti-goat IRDye 800CW, anti-mouse IRDye 800CW, and anti-rabbit IRDye 680 (LI-COR Biosciences, Lincoln, NE), goat Alexa Fluor488-conjugated anti-mouse immunoglobulin G (IgG), and donkey Alexa Fluor568-conjugated anti-goat IgG (Invitrogen).

Cell Culture and Transfection

HeLaM cells stably expressing CD8-CI-MPR were provided by Dr. Matthew N. J. Seaman (University of Cambridge, Cambridge, United Kingdom) and cultured in DMEM containing 500 μg/ml G418 and 10% fetal bovine serum as described previously (Seaman, 2004). HeLa and 293T cells were grown at 37°C in DME supplemented with 1 μg/ml penicillin-streptomycin and 10% fetal bovine serum. 293F cells were maintained at 37°C in FreeStyle 293 expression medium (Invitrogen) and transfected with various plasmids by using 293Fectin reagent (Invitrogen) according to the manufacturer's instructions. To establish the HeLa cells stably expressing GFP-SNX5, the murine ecotropic retrovirus receptor (EcoVR) was first introduced by using the virus produced from BOSC23 cells by transfecting with pCX4hyg-EcoVR, the packaging plasmid pGP, and the envelope plasmid pVSV-G (Akagi *et al.*, 2003; Terai and Matsuda, 2006). After selection by hygromycin, EcoVR-expressing HeLa cells were infected with pMSCVpac-EGFP-SNX5, followed by puromycin selection.

Identification of Interacting Proteins

293T cells were transfected with pCAP-FLAG-DHR1, and binding proteins were analyzed by direct nanoflow liquid chromatography (DNLC)/tandem mass spectrometry (MS/MS) as described previously (Natsume *et al.*, 2002). Briefly, the samples were processed under a stable flow using DNLC. This consists of the following components: a high-pressure syringe pump (KYA Technologies, Tokyo, Japan), a gradient device consisting of 10-channel solvent reservoirs (Valco, Houston, TX), a high-pressure pump mixing module (Hewlett Packard, Palo Alto, CA), and an electrospray ionization column packed with 1-μm reversed-phase beads (Kanto Chemical, Tokyo, Japan). Samples processed through DNLC were injected at flow rates of 25–500 nl/min, and tandem mass spectra were obtained.

Pull-Down Assay and Immunoprecipitation

Twenty-four hours after transfection, 293F cells were washed with Tris-buffered saline (TBS) and lysed with ice-cold lysis buffer (10 mM Tris-HCl, pH 7.5, 5 mM EDTA, 1% Triton X-100, 10 mM NaF, 1 mM Na_3VO_4, 2 mM phenylmethylsulfonyl fluoride, and 10 μg/ml aprotinin). The cleared lysates were incubated with glutathione-Sepharose beads (GE Healthcare, Little Chalfont, Buckinghamshire, United Kingdom) at 4°C for 30 min. After wash-

ing with ice-cold lysis buffer, proteins bound to beads were separated by SDS-polyacrylamide gel electrophoresis (PAGE) and transferred to a polyvinylidene difluoride membrane, followed by detection with antibodies described above. The bound antibodies were detected by an enhanced chemiluminescence detection system (GE Healthcare), and binding was quantified with the aid of an LAS-1000 image analyzer (Fuji Film, Tokyo, Japan). In some experiments, LI-COR Odyssey infrared imaging system scanner (LI-COR Biosciences) was used. For immunoprecipitation, GFP-SNX5–expressing HeLa cells were lysed in lysis buffer and incubated with anti-GFP antibody at 4°C for 60 min, followed by incubation with protein A/G-Sepharose beads (GE Healthcare). The precipitates were processed similarly as described above.

Lipid Binding Assay

293T cells were transfected with various plasmids by 293Fectin (Invitrogen). Forty-eight hours later, cells were collected and lysed in lipid-binding buffer (50 mM Tris-HCl, pH 7.4, 100 mM NaCl, 1 mM EDTA, 0.1% Triton X-100, 5 μg/ml aprotinin, and 1 mM PMSF) on ice. The amount of GFP-tagged proteins was quantified by SDS-PAGE and Western blotting with anti-GFP antibody (Clontech), and the same amount of proteins was diluted by the lipid-binding buffer and incubated to beads conjugated by Di-C_6 or Di-C_6 PIP_3 (Echelon, San Diego, CA). After 6–8 h, the beads were washed twice with lipid washing buffer, 50 mM HEPES, pH 7.4, 150 mM NaCl, 0.25% NP-40, and separated by SDS-PAGE. The proteins bound to the beads as well as normalized total cell lysates were visualized by Western blotting with anti-GFP antibody. Similarly, 293F cells were transfected with several combinations of pCA-EGFP-DOCK180 and pCA-FLAG-SNX5, and they were further analyzed using beads coated with various lipids.

In Vitro Binding Assay

Recombinant proteins fused with glutathione-S-transferase (GST) were expressed in *Escherichia coli* JM109 transformed by pGEX-6P3-SNX5 and pGEX-4T3-DHR1 and purified by the use of Akta*prime* (GE Healthcare). To obtain SNX5, GST-SNX5 was treated with Prescission protease (GE Healthcare). The quality and quantity of proteins were confirmed by SDS-PAGE and Coomassie Brilliant Blue (CBB) staining. Purified SNX5 and GST-DHR1 or GST proteins were incubated with glutathione-Sepharose beads at room temperature for 20 min. After washing with PBS twice, the precipitates were subjected to SDS-PAGE, and bound SNX5 protein was detected by Western blotting using anti-SNX5 antibody.

RNA Interference

Small interfering RNA (siRNA) oligonucleotides against human DOCK180 and Rac1 were purchased from Dharmacon RNA Technologies (Lafayette, CO). The sequences were as follows. DOCK1-1: sense, 5′-GUACCGAGGUUACACGUUAUU-3′; DOCK1-2: sense, 5′-GAAAGUCGAUGGUGGUGAAUU-3′; DOCK1-3: sense, 5′-UAAAUGAGCAGCUGUACAAUU-3′; DOCK1-4: sense, 5′-GGCCCAAGCCUGACUAUUU-UU-3′; Rac1-1: sense, 5′-UAAGGAGAUUGGUGCUGUAUU-3′; Rac1-2: sense, 5′-AGACGGAGCUGUAGGUAAAUU-3′; Rac1-3: sense, 5′-UAAAGACACGAUCGA-GAAAUU-3′; and Rac1-4: sense, 5′-CGGCACCACUGUCCCAACAUU-3′.

siRNA against SNX5 (5′-CGCUCAGUGAGAGAGACAAAGUCAA-3′) and SNX1 (5′-ACUCUAGUCAACCAUAGGA-3′) were from Gene Design (Osaka, Japan; Gullapalli *et al.*, 2004). SOS2 oligonucleotide (sense, 5′-GCCUUUGCUAGAAAAUGCAGAAACU-3′; iGENE Therapeutics, Tsukuba, Japan) was used as a negative control. Cells were seeded at a density of 1×10^4 cells per well on a noncoated 24-well plate (Nalge Nunc International, Rochester, NY) the day before transfection, and they were transfected with siRNA oligonucleotides using RNAi MAX (Invitrogen) according to the manufacturer's protocol. Forty-eight hours after transfection, the cells were processed for immunostaining for CD8-CI-MPR, TGN46, and EEA1, or they were lysed in lysis buffer and subjected to SDS-PAGE and Western blotting to confirm protein depletion.

Immunostaining and Immunofluorescence Microscopy

HeLa and CD8-CI-MPR–expressing HeLaM cells were plated on collagen-coated 35-mm glass-bottomed dishes (Iwaki Glass, Tokyo, Japan) and treated with siRNA as described previously. Forty-eight hours after transfection, cells were fixed in 4% paraformaldehyde/phosphate-buffered saline (PBS) for 10 min at room temperature and permeabilized with 0.1% Triton X-100/PBS for 10 min. After incubation in 10% fetal bovine serum/PBS, cells were incubated with primary antibodies for 1 h, followed by incubation with fluorescent-conjugated secondary antibodies for 1 h at room temperature. To release cytoplasmic proteins, 48 h after transfection, HeLa cells plated on polyethyleneimine-coated 35-mm glass-bottomed dish were treated with 0.001% saponin at room temperature for 5 min before fixation. Fluorescent images were obtained by inverted epifluorescence microscopy by using an IX71 or IX81 microscope (Olympus, Tokyo, Japan) and processed and analyzed by MetaMorph software (Molecular Devices, Sunnyvale, CA). In some experiments, cells were imaged with an FV-500 or -1000 confocal microscope equipped with an Argon and HeNe laser (Olympus).

Anti-CD8 Antibody Uptake Experiment

An anti-CD8 antibody uptake experiment was performed as described previously (Carlton *et al.*, 2005). Briefly, HeLaM cells were plated on collagen-coated 35-mm glass-bottomed dishes and transfected with various siRNA oligonucleotides at a concentration of 1 nM. After 48 h, cells were washed and incubated with DHB buffer (DMEM containing 25 mM HEPES and 0.2% bovine serum albumin) at 4°C for 15 min and labeled with 10 ng/μl anti-CD8 antibody in DHB buffer for 1 h at 4°C. After washing at 4°C with DHB buffer, cells were incubated with prewarmed DMEM containing 10% fetal bovine serum at 37°C to allow internalization of CD8-CI-MPR from the cell surface. Thirty minutes after internalization, cells were washed in ice-cold PBS and fixed and stained with Alexa Fluor488-conjugated secondary antibody. TGN was visualized using anti TGN46 antibody followed by Alexa Fluor568-conjugated secondary antibody. To express the CD8-CI-MPR internalized from cell surface and trafficked to TGN, two images of TGN46 and intracellular CD8-CI-MPR were obtained using epifluorescence microscopy. After subtraction of background intensity, binary images of TGN46 and CD8 were obtained using arbitrary threshold. TGN46 image was overlaid on the CD8 image, yielding the area where CD8-CI-MPR colocalizes with TGN46. The nuclear area was excluded from analysis in all the images because of nonspecific staining of the secondary antibodies in the nuclei. The obtained CD8 area within TGN46 was divided by the total CD8-CI-MPR area within the cells, and then used as the index of CD8-CI-MPR transported to TGN. Whole CD8 area within cells was divided by cell area and used as the CD8-CI-MPR internalized from cell surface. Alternatively, cells were incubated with mouse Alexa Fluor488-conjugated anti-CD8 antibody to follow CD8-CI-MPR, and anti-Golgin97 antibody was used to mark the Golgi apparatus. Obtained images were processed similarly described above; except for that whole cell area was included into analysis to evaluate total volume of internalized CD8-CI-MPR.

Microinjection

Microinjections were performed under an inverted microscope (Carl Zeiss, Jena, Germany) with a micromanipulator 5171 (Eppendorf, Hamburg, Germany) by using an automated FemtoJet (Eppendorf) and glass microcapillaries (Femtotips; Eppendorf). CD8-CI-MPR–expressing HeLaM cells were plated on collagen-coated 35-mm glass-bottomed dishes at a density of 1×10^5 cells per dish, and 100–200 ng/μl plasmids were microinjected. The injection parameters were kept as follows: P_i, 30 hPa; T_i, 0.1 s; and P_c, 30 hPa. Cells were incubated for more than 48 h, followed by immunostaining using anti-CD8 antibody as described above.

RESULTS

SNX5 Is a Novel Binding Partner of the DHR1 Domain of DOCK180

To understand the function of the DHR1 domain, we searched for cellular proteins that physically associate with DHR1 in mammalian cells. For this purpose, FLAG-DHR1 (amino acids 422-664) was expressed in 293T cells and immunoprecipitated from cell lysates with anti-FLAG antibody. The immunoprecipitates were eluted with FLAG peptides, digested with Lys-C endopeptidase, and analyzed using a highly sensitive direct nanoflow LC-MS/MS as described previously (Natsume *et al.*, 2002). A database search identified nine proteins that interact with DHR1, as shown in Table 1. Among the listed proteins,

Table 1. Detection of SNXs as binding partner of DOCK180

Protein name	Results[a]
Sorting nexin1	2/2
Sorting nexin2	2/2
Sorting nexin5	2/2
Sorting nexin6	2/2
Proteasome subunit, α type, 1; isoform unknown	2/2
Prostaglandin E synthase 2; isoform unknown	2/2
Cyclophilin family	1/2
Proteasome subunit, α type, 7 family	1/2
Proteasome 26S subunit, non-ATPase, 2	1/2

[a] Positive results/total experiments.

SNX1, 2, 5, and 6 were found to associate with DHR1 repeatedly, validating further analyses.

To confirm the binding of DHR1 to SNXs, 293F cells were transfected with plasmids for GST-tagged DHR1 and FLAG-tagged SNXs (Figure 1A). GST-DHR1 collected on glutathione-Sepharose was found to associate with SNX5. After a long exposure of the filter, we could detect the interaction of DHR1 to other SNXs (data not shown). Because recent studies have shown that SNXs form homo- and hetero-oligomers (Parks *et al*., 2001; Liu *et al*., 2006), we examined whether SNX5 was associated with other SNXs in our experimental condition (Supplemental Figure S1A). We found that SNX5 associated with SNX1 and SNX2, and also with SNX6, albeit to a lesser extent. These data suggest that DHR1 directly binds to SNX5 and indirectly to SNX1, 2, and 6 via SNX5.

SNX5 Specifically Interacts with DOCK180

DOCK180 belongs to the DOCK180 superfamily, which contains at least 11 human DOCK180 homologues and several homologous members in other species. The binding of SNX5 to the DHR1 domain of other DOCK180 members was examined in 293F cells (Supplemental Figure S1B). Among the tested DHR1 domains of DOCK180 family proteins—DOCK2, DOCK3, DOCK4, DOCK6, and DOCK9—only the DHR1 domain of DOCK180 showed binding to SNX5 to a detectable level. To examine whether the full-length DOCK180 also interacts with SNX5, GST-tagged SNX5 and FLAG-tagged DOCK180 or DHR1 were expressed in 293F cells, followed by pull-down analysis with glutathione-Sepharose. As shown in Figure 1B, the full-length DOCK180 bound to SNX5 as did DHR1.

We next examined the interaction between DOCK180 and SNX5 at the physiological expression level. Before this analysis, we quantified the molecule numbers of the endogenous DOCK180, SNX1, and SNX5 in HeLa cells essentially as described previously (Aoki *et al*., 2007) (Table 2 and Supplemental Figure S2). We found that DOCK180 is ~10 times fewer than SNXs. Because the SNX5 antibody used in this study could not immuno-precipitate SNX5 efficiently, we failed to detect DOCK180 in the immune complex (data not shown). To overcome this, we established HeLa cells stably expressing GFP-SNX5. In these GFP-SNX5–expressing cells, the expression level of the endogenous SNX5 protein was decreased (Figure 1C). When the amount of endogenous and exogenous SNX5s was quantified in these cells, the sum of endogenous and exogenous SNX5s in the GFP-SNX5–expressing cells was ~1.5 times as much as the endogenous SNX5 in the parental cells. Using these cells, we could show the coprecipitation of endogenous DOCK180 with the GFP-SNX5 protein (Figure 1D), indicating that the expression levels of endogenous SNX5 and DOCK180 are sufficient to form the SNX5–DOCK180 complex.

To demonstrate direct interaction of DHR1 and SNX5, we prepared GST-tagged DHR1 and SNX5 expressed in *E. coli*. GST-SNX5 was further cleaved by a protease to remove GST-tag. With these recombinant proteins, we found that SNX5 was coprecipitated with GST-DHR1, but not with GST alone, demonstrating the direct interaction of DHR1 with SNX5 (Figure 1E).

DOCK180 Localizes to Endosomes with SNX5

Previously, it has been reported that the localizations of SNX5 and DOCK180 are early endosomes and cytoplasm, respectively (Hasegawa *et al*., 1996; Teasdale *et al*., 2001). To examine SNX5 and DOCK180 interaction in the cell, SNX5 and DOCK180 with fluorescent proteins were expressed in HeLa cells, and observed with confocal microscopy (Figure 2A). As reported previously, GFP-DOCK180, as well as GFP and red fluorescent protein (RFP), is localized in the cytoplasm, whereas GFP- and RFP-SNX5 localized to the vesicles in the fixed cells. Because we anticipate that abundant DOCK180 in the cytoplasm perturbs observation of DOCK180 at the vesicles, cells expressing RFP-SNX5 and GFP-DOCK180 were treated with 0.001% saponin before fixation to release cytoplasmic proteins from the cells (Figure 2B). Although SNX5 localized mainly to the vesicles, DOCK180 localized both to cytoplasm and vesicles, which are merged to SNX5, suggesting that a small fraction of DOCK180 binds to SNX5.

The First Helix of the SNX5 Bin/Amphiphysin/Rvs (BAR) Domain Is Necessary for Binding to DHR1

SNX5 contains the N-terminal PX domain (amino acids 64–168) and the C-terminal coiled-coil region encoding the BAR domain (206-397) (Figure 3A) (Merino-Trigo *et al*., 2004). SNXs are subgrouped into seven classes based on their amino acid sequence similarity of PX domain (Worby and Dixon, 2002). The SNX5, together with SNX1, SNX2, and SNX6, is classified into the same group. X-ray crystallography has revealed that the BAR domain conforms to a coiled-coil structure consisting of three α helices, 1–3 (Peter *et al*., 2004). To identify the helix responsible for the DHR1 binding, we first attempted to express each helix alone, but they were all insoluble or unstable in tissue culture cells. Thus, in the following experiment we used C-terminal–truncated mutants as schematically shown in Figure 3A. Comparable expression levels of these FLAG-tagged SNX5 mutants were confirmed in 293F cells (Figure 3B). Next, we examined the binding of GST-DHR1 to these truncated mutants. As shown in Figure 3C, truncated mutants containing the first and second helices of the BAR domain associated with DHR1 to a similar extent as the full-length SNX5. When all of the BAR domains was deleted from SNX5 in the PX mutant, SNX5 did not associate with DHR1. Although the insolubility of the BAR domain prevented us from directly evidencing it, the data strongly suggested that the first helix of the BAR domain bound to DHR1. Alternatively, our observation might suggest that the PX domain played an essential role in DHR1 binding, and the first helix of the BAR domain might contribute to this simply by stabilizing the conformation of the PX domain. Regardless, we concluded that the first helix of the BAR domain was necessary for association with DHR1.

DOCK180 Deficiency Alters the Distribution of CI-MPR

SNX1 is a component of the retromer complex, which functions in the retrieval process of CI-MPR from early endosome to TGN (Carlton *et al*., 2004). The RNAi loss-of-function screen of SNXs has identified SNX5 and SNX6 as potential components of the retromer (Wassmer *et al*., 2007). These observations prompted us to examine whether DOCK180 is involved in this retrograde transport of CI-MPR through the binding to SNX5. Previous studies have shown that knockdowns of SNX1 and SNX5 induced redistribution of endogenous and CD8-tagged CI-MPR from TGN to endosomes. When this CD8-CI-MPR-reporter protein, consisting of the extracellular domain of CD8 and the cytoplasmic domain of bovine CI-MPR, is expressed in HeLa cells, it cycles between endosomes and TGN (Seaman, 2004). During this cycle, the retromer regulates the retrieval of CD8-CI-MPR from endosome to TGN. We examined whether the DOCK180 knockdown altered the steady-state distribution of CD8-CI-MPR, as did that of SNX5. HeLaM cells, which constitutively express CD8-CI-MPR, were transfected with siRNA duplexes against DOCK180, SNX5, and SOS2 (Figure

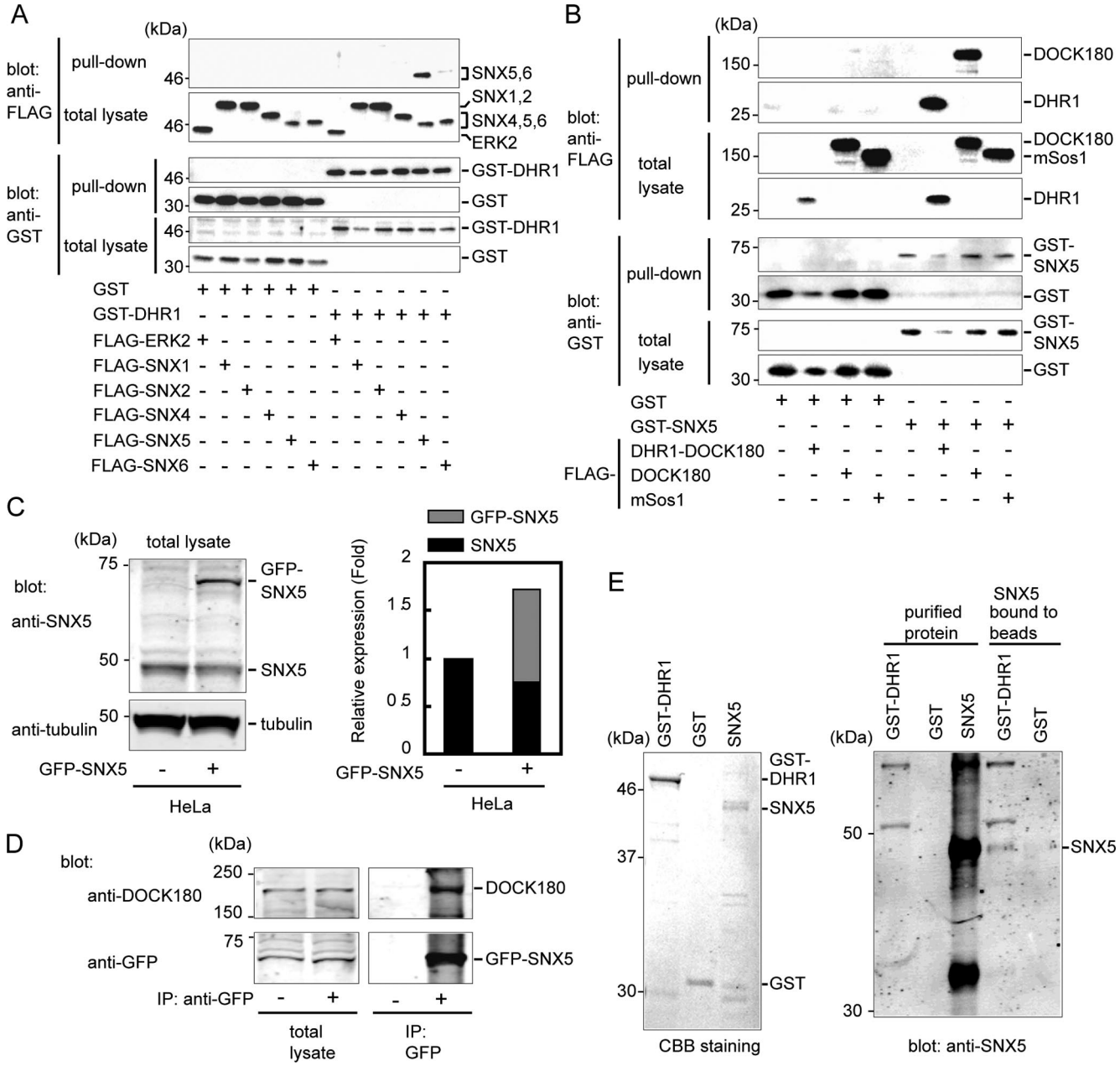

Figure 1. DOCK180 binds to SNX5. (A) 293F cells were transfected with various combinations of plasmids for proteins indicated at the bottom. After 24 h, cells were lysed and supernatants were incubated with glutathione-Sepharose. After the beads were washed with ice-cold lysis buffer, bound proteins (denoted as pull-down) as well as total lysate were separated by SDS-PAGE and detected by Western blotting with antibodies against FLAG and GST indicated to the left. The corresponding bands to ERK2, SNXs, GST, and GST-DHR1 are denoted to the right. Three independent experiments demonstrated similar results. (B) 293F cells were cotransfected with various combinations of plasmids encoding proteins as indicated at the bottom. Cells were processed and analyzed as described for A. The corresponding bands to DOCK180, DHR1, mSos1, GST-SNX5, and GST are denoted to the right. (C) Establishment of GFP-SNX5 expressing HeLa cells. Lysates from the parental (left lane) and GFP-SNX5 expressing (right lane) HeLa cells were subjected to SDS-PAGE and Western blotting using indicated antibodies. The corresponding bands to endogenous or GFP-tagged SNX5 and tubulin are indicated to the right. The intensities of endogenous and exogenous SNX5 bands in GFP-SNX5–expressing cells were divided by that of endogenous SNX5 in the parental cells and shown in the graph. Black and gray bars represent endogenous and GFP-tagged SNX5, respectively. (D) Binding of endogenous DOCK180 to GFP-SNX5. GFP-SNX5 expressing HeLa cells were lysed and supernatants were incubated with anti-GFP antibody. Proteins were collected by protein A/G-Sepharose beads, separated by SDS-PAGE, and detected with indicated antibodies. Bands corresponding to DOCK180 and GFP-tagged SNX5 are indicated to the right. IP, immunoprecipitate. (E) In vitro binding of GST-DHR1 and SNX5. GST-DHR1, GST, and SNX5 protein were expressed in *E. coli* and purified. GST-SNX5 was cleaved with a protease to obtain SNX5 without GST. The proteins were separated by SDS-PAGE, stained with CBB. The corresponding bands to GST-DHR1, GST, and SNX5 are indicated to the right (left). SNX5 and GST-DHR1 or GST proteins were incubated with glutathione-Sepharose beads at room temperature for 20 min and separated by SDS-PAGE. The bound SNX5 protein was detected by Western blotting using anti-SNX5 antibody (right).

Table 2. Number of DOCK180, SNX1, and SNX5 in HeLa cells

	No. (/cell)
DOCK180	3.9×10^5
SNX1	4.3×10^6
SNX5	3.0×10^6

HeLa cells were transfected with plasmids for GFP-DOCK180, -SNX1, and -SNX5 and lysed in lysis buffer. Proteins were separated by SDS-PAGE and detected by Western blotting with anti-GFP antibody. GST-5myc-FLAG-3HA-YFP protein was expressed *E. coli* and used as a standard as described previously (Aoki *et al.*, 2007). The same proteins were examined by Western blotting with antibodies against DOCK180, SNX1, and SNX5 to calculate the numbers of endogenous proteins. The representative images were shown in Supplemental Figure S2. Results obtained from three independent experiments.

4A). The SOS2 siRNA was used as a control. The oligonucleotide treatment at concentrations of both 1 and 5 nM specifically reduced the expression of targeted proteins 48 h after transfection, to 10–20% of that without the treatment (Figure 4B). In parallel, these cells were immunostained with anti-CD8 antibody (Figure 4C). In cells without or with control siRNA treatment, most of the CD8-CI-MPR remained in the perinuclear region, as reported for the endogenous CI-MPR. This perinuclear staining colocalized with

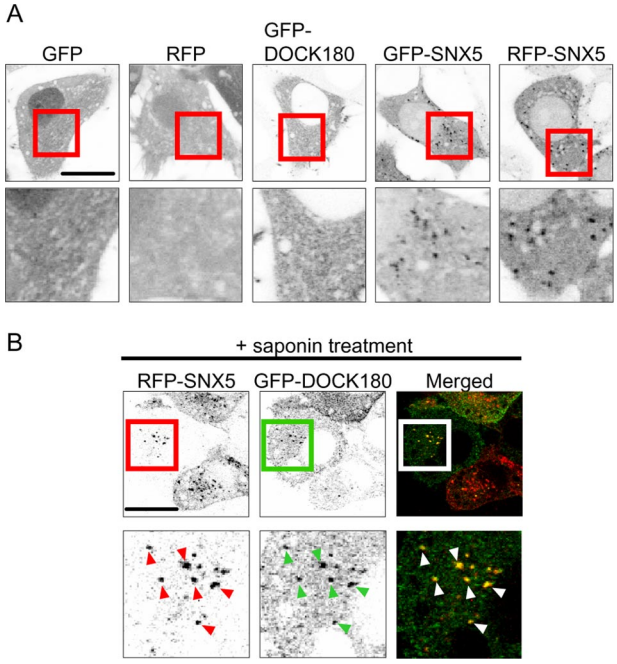

Figure 2. SNX5 and DOCK180 localizes to the vesicles. (A) HeLa cells were transfected with plasmids encoding proteins indicated above. Forty-eight hours later, cells were fixed and imaged by confocal microscopy. Enlarged images from red squares in the top panels are shown at the bottom. Bar, 20 μm. (B) HeLa cells were cotransfected with plasmids for RFP-SNX5 and GFP-DOCK180. Forty-eight hours later, cells were treated with 0.001% saponin for 5 min at room temperature, before fixation. Images were obtained by confocal microscopy. Enlarged images from squares in the top panels are shown at the bottom. Arrowheads indicate colocalization of SNX5 and DOCK180. Bar, 20 μm.

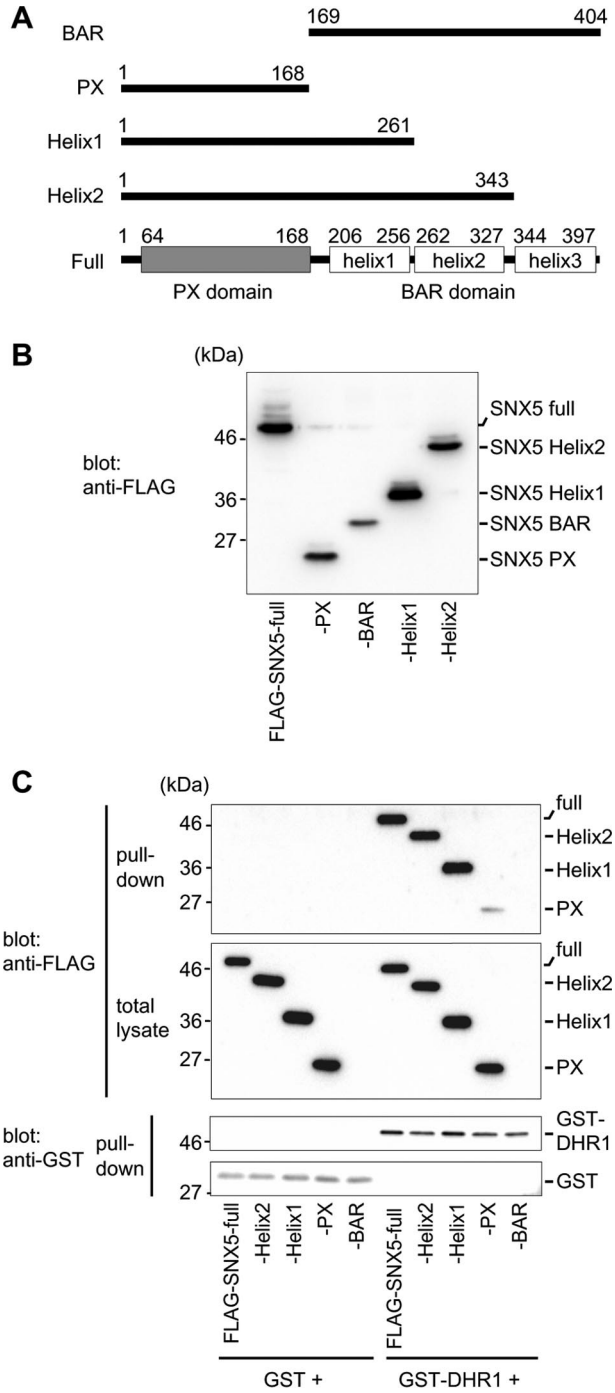

Figure 3. The first helix of the BAR domain is necessary for interaction with the DHR1 domain. (A) Schematic representation of SNX5 mutants. Numbers at the top of each bar indicate the amino acid numbers of human SNX5. The domains corresponding to PX, BAR, and helices 1–3 are shown in the full (that is, the wild type) at the bottom. The BAR domain consists of three helices, 1–3. (B) 293F cells were transfected to express proteins indicated at the bottom. Twenty-four hours later, cells were collected and directly lysed in SDS-sample buffer. Proteins were separated by SDS-PAGE and examined by Western blotting with anti-FLAG antibody. The corresponding bands to full-length and mutants of SNX5 are denoted to the right. (C) 293F cells transiently expressing the proteins indicated at the bottom were analyzed as in Figure 1A. The bands corresponding to the full-length and mutants of SNX5, GST, and GST-DHR1 are denoted to the right. Three independent experiments demonstrated similar results.

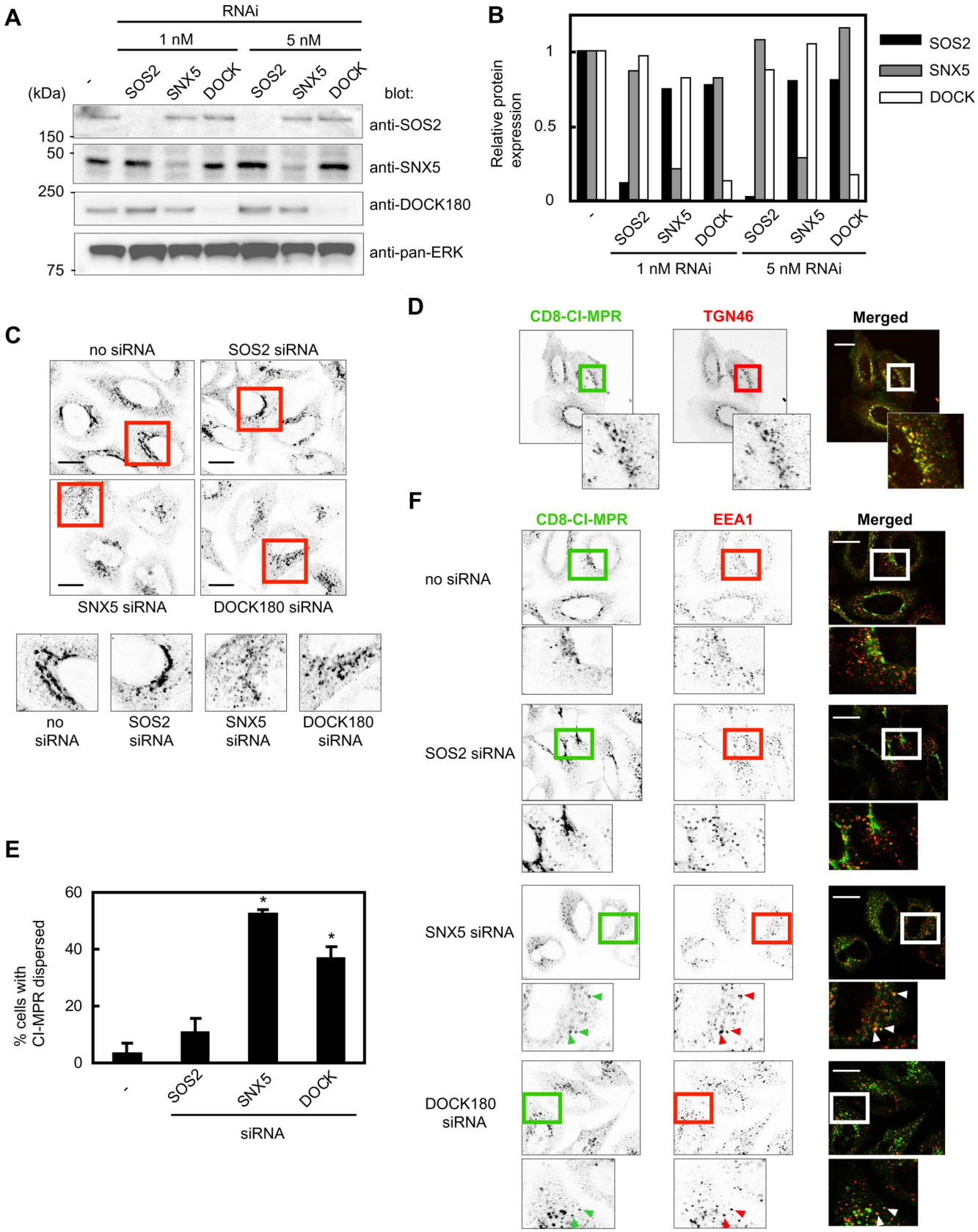

Figure 4. Suppression of DOCK180 alters steady-state distribution of the CI-MPR. (A) CD8-CI-MPR–expressing HeLaM cells were treated for 48 h with SOS2-, SNX5-, or DOCK180-targeted siRNA oligonucleotides (indicated at the top), in a concentration of 1 or 5 nM, and examined for protein depletion by SDS-PAGE and Western blotting with antibodies against SOS2, SNX5, DOCK180, and pan-ERK as indicated to the right. (B) Suppression of SOS2, SNX5, and DOCK180 proteins was quantified from Western blotting in A. The intensities of

that of a TGN marker, TGN46 (Figure 4D). In contrast, the knockdown of SNX5 or that of DOCK180 dispersed the CD8-CI-MPR at TGN, resulting in the formation of a peripheral punctate structure (Figure 4C, bottom). To quantify the degree of CD8-CI-MPR redistribution caused by DOCK180 or SNX5 deficiency, cells were divided into two typical phenotypes according to the CD8-CI-MPR distribution (Supplemental Figure S3): 1) the TGN pattern and 2) the dispersed pattern showing peripheral punctate localization. In DOCK180-deficient cells, 36.8 ± 4.2% of cells showed a dispersed pattern of CD8-CI-MPR, which was less than that observed in SNX5 knockdown cells (Figure 4E) but significantly higher than that in the control cells ($p < 0.05$). Because this morphological classification is liable to fluctuation, we performed a blind test in which three pathologists classified the stained cells into either TGN or the dispersed pattern without any information on the transfected siRNA (Supplemental Figure S4). Although the absolute numbers varied among the three examiners, all examiners reached the same conclusion: the dispersed pattern of CI-MPR occurs most frequently in SNX1-depleted cells, and, to a lesser extent, in DOCK180-depleted cells. To examine the subcellular localization of the dispersed CI-MPR in DOCK180-deficient cells, cells were stained with an early endosomal marker, EEA1 (Figure 4F). In control cells, CD8-CI-MPR was mainly localized to TGN. In contrast, in cells treated with siRNA oligonucleotides against SNX5 and DOCK180, the peripheral CD8-CI-MPR-labeled structures exhibited partial colocalization with EEA1. These data strongly supported our view that DOCK180 regulates the retrograde transport of CI-MPR similarly to SNX5.

Internalization and Trafficking of CD8-CI-MPR Are Disturbed in DOCK180-deficient Cells

To examine whether the alteration in the steady-state distribution of CD8-CI-MPR resulted from a perturbation in the kinetics of early endosome-to-TGN transport, we examined the uptake of anti-CD8 antibodies. HeLaM cells were treated with siRNAs as described above, and they were incubated with anti-CD8 antibody at 4°C to label CD8-CI-MPR expressed on the plasma membrane, followed by warming to 37°C for 30 min to allow its internalization from the cell surface. The CD8-CI-MPR was transported through the early endosome, and the bulk reached TGN by the time of observation. After 30-min incubation, most of the CD8-CI-MPR was found to be localized to TGN in control cells, whereas significantly less CD8-CI-MPR was observed within TGN and instead distributed in peripheral vesicular structure in the SNX5- or DOCK180-deficient cells (Figure 5A). Because retromer regulates cargo protein sorting from endosome to TGN, the retromer function can be monitored by the level of CD8-CI-MPR that has been retrieved to TGN (Carlton *et al.*, 2005). For this, we measured the total area of CD8-CI-MPR showing the colocalization with TGN46 as described in *Materials and Methods*. Although the total area of internalized CD8-CI-MPR was at similar level in control cells and SNX5- or DOCK180-depleted cells (Figure 5B, left column), the CD8-CI-MPR reached to TGN was less in both SNX5- or DOCK180-depleted cells (Figure 5B, right column). Furthermore, a previous study has shown that SNX5 knockdown induces TGN fragmentation (Wassmer *et al.*, 2007). We confirmed this observation (Figure 5C) and found that DOCK180 knockdown induced similar TGN fragmentation, further supporting our view that DOCK180 cooperates with SNX5. Instead of TGN46, another marker for the TGN, Golgin97, was used to show that the distribution of Golgin97 was not affected by siRNA treatment against SNX5 and DOCK180 (Figure 5D). We quantified the CD8-CI-MPR trafficking inhibition under this condition, to find that the transport of CD8-CI-MPR to TGN marked by Golgin97 was affected more severely than that to TGN marked by TGN46 (Figure 5E).

Depletion of Rac1 Did Not Affect CI-MPR Transport

An established function of DOCK180 is to activate Rac1, which regulates actin organization (Kiyokawa *et al.*, 1998a). A recent study has demonstrated the retromer-component proteins VPS26 and VPS35 localized to ruffles at the plasma membrane, which are rich in polymerized actin (Kerr *et al.*, 2005). To address the question of whether Rac1 is required for CI-MPR trafficking, HeLaM cells were treated with siRNA duplexes against Rac1 for 48 h to reduce protein expression to an undetectable level (Figure 6A). In these Rac-deficient cells, the steady-state distribution of CD8-CI-MPR examined as in Figure 4E was similar to that of the control cells, negating the involvement of Rac1 in CI-MPR localization (Figure 6B).

RLC Mutation in DHR1 Ablates the DOCK180 Binding to SNX5 and Phosphoinositide

Recently, a 27-base pair deletion in the DHR1 domain of mouse DOCK5 was discovered in a RLC mutant, a hereditary cataract in mice (Omi *et al.*, 2008). We introduced this deletion, corresponding to amino acids 488–496, into DHR1 of human DOCK180, and we examined its binding to SNX5. As shown in Figure 7A, RLC deletion of DHR1 diminished the binding to SNX5. This observation indicates that SNX5 binds to DOCK180 through DHR1 and suggests that SNX5 binding is an essential physiological function of DOCK180. Cote *et al.* (2005) have found that DHR1 binds to PIP_3 and $PI(3,5)P_2$, through amino acid residues 422-619. Because RLC mutation is located in the minimal lipid-binding site, we next examined the effect of RLC mutation on the lipid

Figure 4 (cont). SOS2, SNX5, and DOCK180 bands were divided by those of pan-ERK from the same lanes to obtain the normalized intensities. Relative protein expression was calculated by normal intensity from the siRNA-treated sample divided by that from siRNA nontreated sample. The treated siRNA duplexes are indicated at the bottom of the graph. Black, gray, and white bars indicate the relative amounts of SOS2, SNX5, and DOCK180, respectively. (C) In a parallel experiment in A, siRNA-treated cells were fixed in 4% paraformaldehyde and immunostained with anti-CD8 antibody and Alexa Fluor 488-conjugated secondary antibody. Cell images were acquired with confocal microscopy. Representative image of cells treated with 1 nM siRNA oligonucleotides are shown. Enlarged images from red squares in the top panels are shown at the bottom. Bar, 20 μm. (D) CD8-CI-MPR–expressing HeLaM cells were fixed and stained with anti-CD8 and anti-TGN46 antibodies, followed by Alexa-conjugated secondary antibodies. Cell images were obtained with confocal microscopy. Enlarged images in the insets are shown at the bottom. Bar, 20 μm. (E) Quantitative analysis of percentage of cells with CI-MPR dispersed in siRNA-treated cells. Results were obtained from cells treated with 1 nM and 5 nM of siRNA oligonucleotides as two independent experiments. Representative images for quantitative analysis are shown in Supplemental Figure S3. More than 50 cells were counted in all experiments, and mean ± SD percentage of cells with dispersed CI-MPR is shown. Asterisks indicate the significance of *t* test analysis: $^*p < 0.05$ (vs. control siRNA). (F) CD8-CI-MPR-expressing HeLaM cells were fixed and stained with anti-CD8 (left) and EEA1 (middle) antibodies. Cell images were obtained by confocal microscopy. Treated siRNA duplexes are denoted to the left. Bar, 10 μm. Enlarged images from green and red squares in the top panels are shown at the bottom. Arrowheads indicate vesicles where CD8-CI-MPR and EEA1 are colocalized.

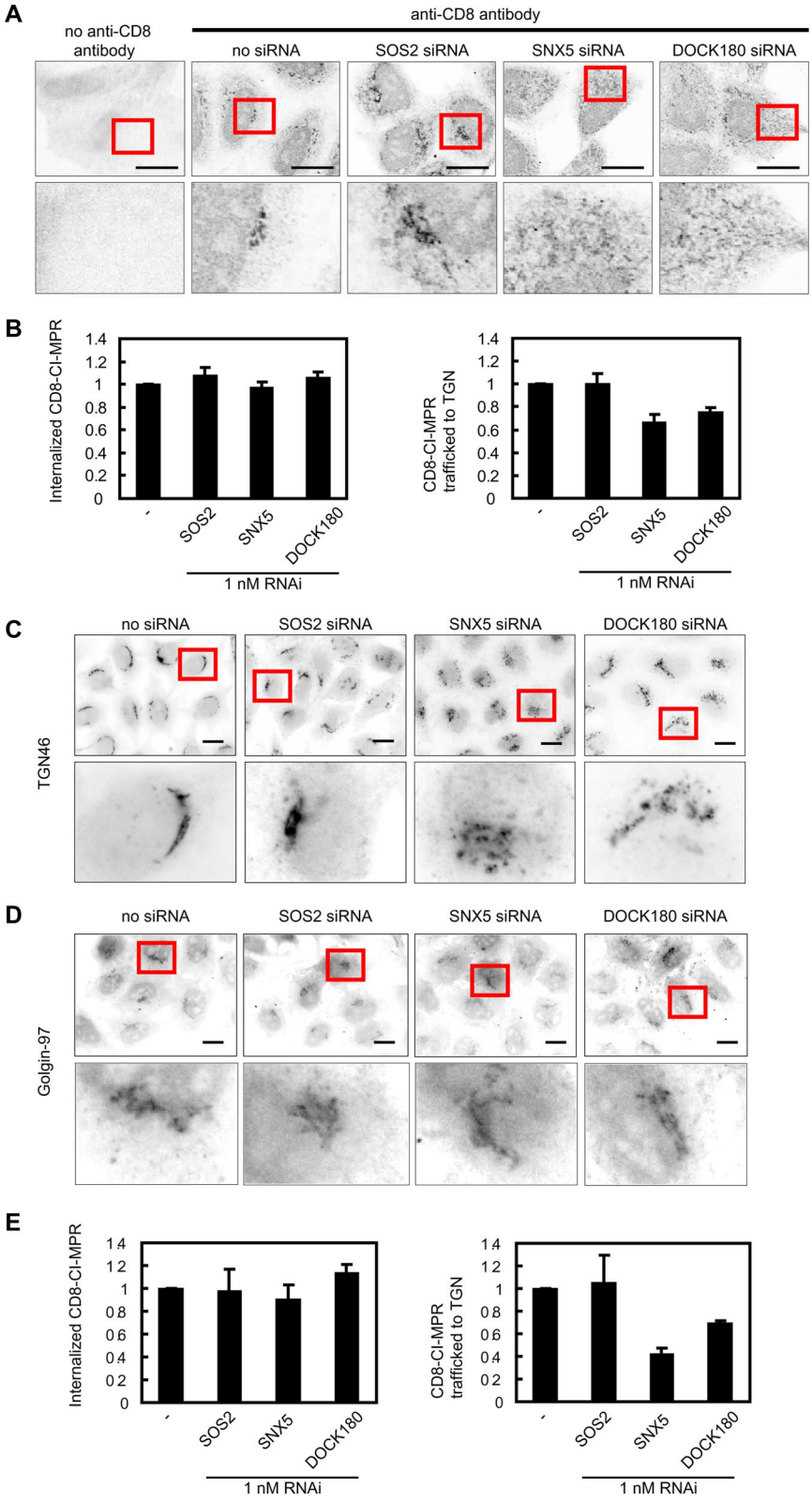

Figure 5. Kinetics of CD8-CI-MPR is altered in DOCK180-suppressed cells. (A) CD8-CI-MPR–expressing HeLaM cells were treated with 1 nM SOS2-, SNX5-, or DOCK180-targeted siRNA oligonucleotides. Forty-eight hours later, cells were incubated with anti-CD8 antibody at 4°C for 1 h. After labeling, cells were warmed up to 37°C, incubated for 30 min, and fixed (denoted as 30 min to the left). Cells were then stained with Alexa Fluor488-conjugated secondary antibody, and images were obtained with confocal microscopy. Representative images of CD8-CI-MPR–expressing HeLaM cells treated with siRNA oligonucleotides indicated at the top were shown. For negative control for staining, cells without siRNA treatment were processed similarly but without anti-CD8 antibody (left column). Enlarged images from red squares in the top panels are shown at the bottom. Bar, 20 μm. (B) Quantitative analysis of CD8-CI-MPR internalized from cell surface (left) and trafficked to TGN (right panel) as described in *Materials and Methods*. Data are shown as a relative amount of CD8-CI-MPR compared with no-siRNA oligonucleotides treated cells and expressed as mean ± deviation form two independent experiments. More than 30 cells were analyzed in each experiment. (C) In the parallel experiment in A, TGN was visualized with epifluorescence microscopy, and representative images of cells treated with siRNA oligonucleotides indicated at the top are shown. Enlarged images from red squares in the top panels are shown at the bottom. Bar, 20 μm. (D) siRNA-treated CD8-CI-MPR–expressing HeLaM cells were immunostained with anti-Golgin97 antibody and Alexa Fluor488-conjugated secondary antibody. Images were obtained and shown as in C. Bar, 20 μm. (E) Quantitative analysis of anti-CD8 uptake assay using mouse Alexa Fluor488-conjugated anti-CD8 and anti-Golgin97 antibodies and as described in *Materials and Methods*. Data from two independent experiments are shown as in (B). In each experiment, 15–27 cells were analyzed. Bar represents mean ± deviation.

recognition of DOCK180. As shown in Figure 7B, the wild-type DOCK180, but not the RLC mutant, bound to PIP_3, as described previously (Kobayashi *et al.*, 2001; Cote *et al.*, 2005). To investigate whether SNX5 competes with PIP_3 for the binding to DOCK180, DOCK180 in the presence or absence of SNX5 were incubated with the beads coated with PIP_3 or $PI(4,5)P_2$ (Figure 7C). The amounts of DOCK180 bound to the PIP_3 beads were not changed in the presence or absence of SNX5, as shown in the first and second rows. Furthermore, SNX5 was found to be coprecipitated with

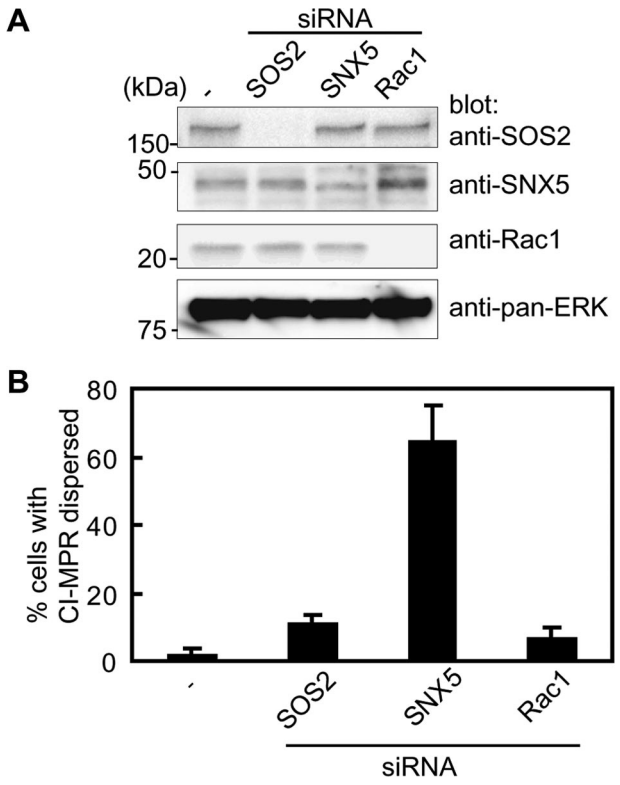

Figure 6. Rac1 does not affect steady state CI-MPR distribution. (A) CD8-CI-MPR–expressing HeLaM cells were treated with 1 nM of SOS2-, SNX5-, or Rac1-targeted siRNA oligonucleotides indicated at the top. Forty-eight hours later, proteins were examined by Western blotting with antibodies against SOS2, SNX5, Rac1, and pan-ERK as indicated to the right. (B) In parallel, cells were processed and analyzed as in Figure 4, C and E. Percentage of cells with dispersed CI-MPR was calculated, and mean ± SD from three independent experiments is shown.

PIP_3-coated beads only in the presence of DOCK180. Although we could not perform similar experiments with $PI(3,5)P_2$ due to a technical problem, these data suggest that DOCK180 bridges the SNX5-bearing protein complexes to the membranes rich in PIP_3 or $PI(3,5)P_2$.

DHR1 Is Sufficient for CI-MPR Transport

Last, we challenged the question of whether or not DHR1 is sufficient for the role that DOCK180 plays in CD8-CI-MPR transport. We prepared pSuper-DOCK180, a vector-based shRNA targeting DOCK180, as well as pCA-EGFP-$DOCK180^R$, pCA-EGFP-$DHR1^R$, and pCA-EGFP-$DHR1^R$-RLC, expression vectors for the DOCK180 mRNAs that are resistant to the aforementioned shRNA. Expression levels of these proteins were examined in 293F cells by Western blotting (Supplemental Figure S5). To ensure the coexpression, we microinjected these plasmids into HeLaM cells and examined their effects on CD8-CI-MPR distribution. As expected, shRNA for DOCK180 induced the dispersed CD8-CI-MPR pattern, and this effect of shRNA was ablated by the coexpression of shRNA-resistant DOCK180 (Figure 7D). A similar experiment was conducted with shRNA-resistant DHR1 of DOCK180 (Figure 7E). We found that reexpression of $DHR1^R$ suppressed the shRNA-induced dispersion of CD8-CI-MPR as efficiently as that of the full-length DOCK180. However, expression of shRNA-resistant RLC mutant of DHR1 could not restore the steady-state distribution of CI-MPR in DOCK180-suppressed cells (Figure 7E). Thus, we concluded that DHR1 of DOCK180 is sufficient to regulate the retrograde transport of CI-MPR.

DISCUSSION

In this study, we have identified SNX5 as a novel binding partner of DOCK180 by nano-LC/MS/MS, and we have shown that DOCK180 localizes to the endosome with SNX5 (summarized in Figure 8). Knockdown of either SNX5 or DOCK180 perturbed the CI-MPR transport from early endosome to TGN, suggesting that the binding is physiologically relevant. For this regulation of CI-MPR transport, we found that the DHR1 of DOCK180 was sufficient, and thus it was not necessary for DOCK180 to bind to ELMO, Rac1, or CRK. SNX5 was found to bind to DHR1 of DOCK180, but not to those of other DOCK-family proteins. This high specificity to DOCK180 was surprising in light of previous observations that most, if not all, DOCK-family proteins share GEF activity for Rac1 and/or Cdc42 and the affinity to phosphoinositides (Nishihara *et al.*, 1999; Cote and Vuori, 2002; Watabe-Uchida *et al.*, 2006).

Aberrant CI-MPR transport caused by the knockdown of either SNX5 or DOCK180 supports our view that DOCK180 regulates the retromer complex via its interaction with SNX5 (Figures 4, 5, and 8). The finding that DHR1 recognition requires amino acids 169–261 of SNX5, spanning the N-terminal-linker and the first helix of the BAR domain, may provide a clue to the molecular mechanism (Figure 3). This observation suggests that, either directly or indirectly, DHR1 of DOCK180 may regulate the function of the BAR domain to deliver CI-MPR properly. The BAR domain has been suggested to be involved in dimer formation and curvature sensing. A crystal structure study of the BAR domain from *Drosophila* amphiphysin has revealed that the BAR domain conforms to a homo dimer of two kinked rods arranged at an angle and in the opposite orientation and fits its banana shape into the curvature of the liposomes (Peter *et al.*, 2004). Consistent with this observation, SNX1 has been shown to reside on the tubular elements on the early endosomes, forms the dimer, binds preferentially to a highly curved membrane, and tubulates membranes in vitro (Carlton *et al.*, 2004). More recently, SNX5 has been shown to associate with tubular extensions of the macropinosome (Kerr *et al.*, 2006) and the SNX1-endosome (Wassmer *et al.*, 2007), indicating that the SNX5 BAR-domain also possesses membrane-bending and curvature-sensing capacities. Importantly, we found that DHR1 is sufficient to rescue the aberrant retrograde transport of CI-MPR in DOCK180-deficient cells (Figure 7, D–F). Thus, it is possible that DHR1-binding to the BAR domain of SNX5 may change its conformation suitable for the retrograde transport of CI-MPR.

It remains an open question whether the binding of DHR1 to PIP_3 is required for its regulation of SNX5. However, the observation that the RLC mutation in DHR1 ablated binding to both SNX5 and PIP_3 suggests that DHR1 functions as a molecular glue to recruit the retromer complex from early endosome to the TGN or late endosomes (Figure 8). Notably, DHR1 binds to $PI(3,5)P_2$ as efficiently as PIP_3 (Cote *et al.*, 2005). In contrast to PIP_3, which is primarily found in the plasma membrane, $PI(3,5)P_2$ is enriched at the late endosome (Di Paolo and De Camilli, 2006). Recently, it was revealed that some fraction of MPR is transferred from early to late endosomes in a syntaxin 10-dependent manner (Ganley *et al.*, 2008). Therefore, we could speculate that DHR1 might play a role in retrograde transport by targeting the SNX5 complex to the late endosome. In vitro binding of

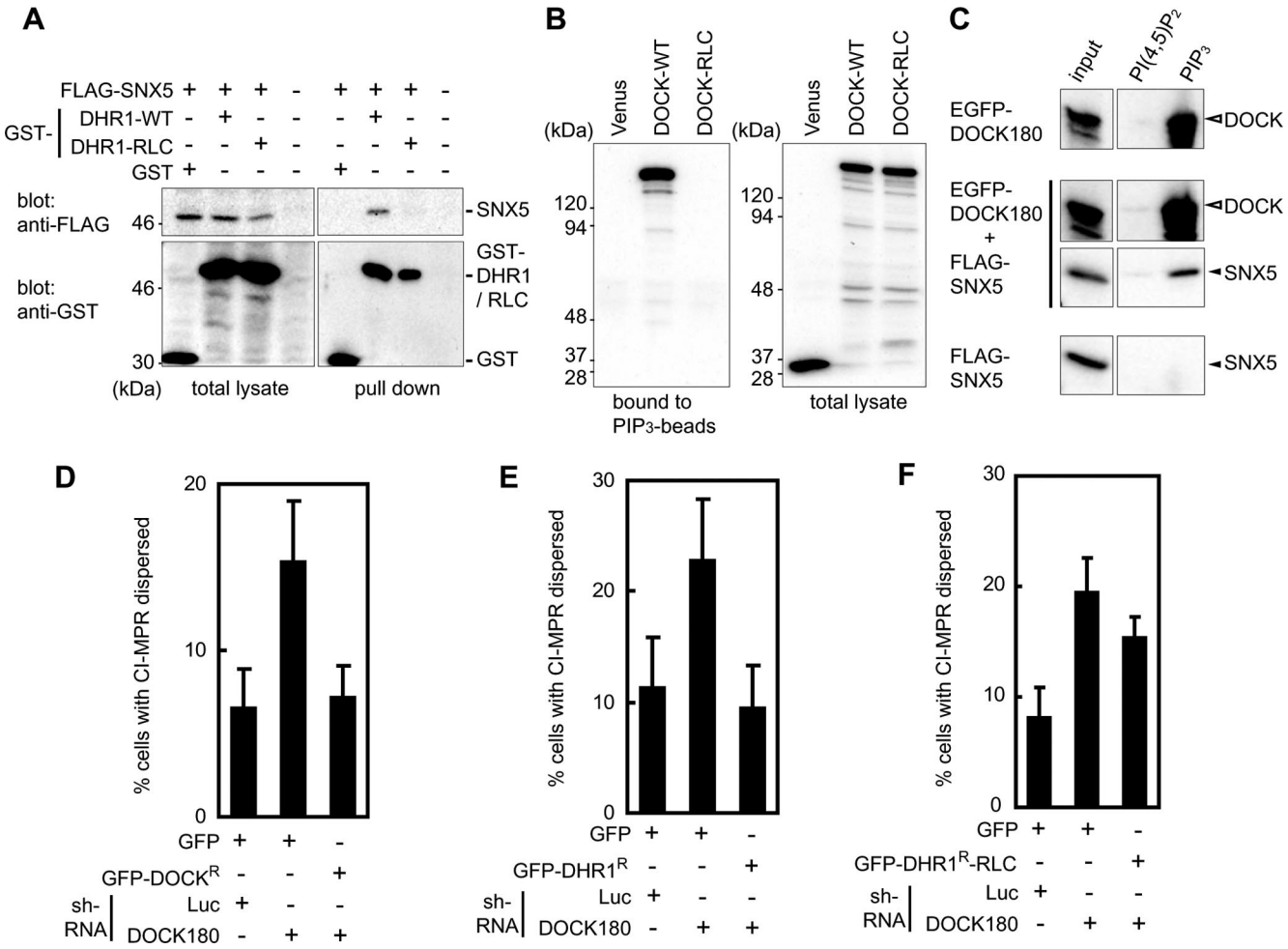

Figure 7. DHR1 of DOCK180 is sufficient for CI-MPR transport. (A) 293F cells were transfected with plasmid encoding proteins indicated at the top and analyzed as described in Figure 1A. WT and RLC denote the wild type and RLC mutant, respectively. The corresponding bands to SNX5, GST, GST-DHR1-WT, and GST-DHR1-RLC are denoted to the right. (B) Plasmids for the Venus-tagged proteins indicated at the top were transfected into 293T cells. Forty-eight hours later, cells were collected and lysed and processed further as described in *Materials and Methods*. The proteins bound to the beads and total cell lysate (denoted as "bound to PIP_3-beads" and "total lysate" at the bottom) occur in the left and right panels, respectively, which were blotted with anti-GFP antibody. The results are representative of three independent experiments. (C) 293F transiently expressing EGFP-DOCK180, FLAG-SNX5, or both, as indicated to the left, were collected and lysed. Proteins were incubated with beads conjugated by the lipids indicated at the top, and bound proteins were analyzed using SDS-PAGE and Western blotting by antibody against FLAG and GFP. White and black arrowheads indicate EGFP-DOCK180 and FLAG-SNX5, respectively, as denoted to the right. (D–F) CD8-CI-MPR–expressing HeLaM cells were microinjected with various combinations of plasmids for proteins and shRNA indicated at the bottom. Forty-eight hours later, cells were processed and analyzed as in Figure 4, C and E. The mean ± SEM from three independent experiments are shown.

the retromer complex in the presence of DHR1 to the reconstituted liposomes will provide the details of these interactions; however, due to the insolubility of the recombinant DHR1 in *E. coli*, this hypothesis has not been tested at this moment.

It has been reported that the constitutive-active form of Rac1 inhibits the internalization of transferrin and EGF receptors from the clathrin-coated pit (Lamaze *et al*., 1996). However, we could not observe the effect of Rac1 knockdown in the transport of CI-MPR at the steady state (Figure 6). This discrepancy suggests that Rac1 regulates the transport from plasma membrane to early endosome but not from early endosome to TGN. Growing evidence suggests that the BAR domain-mediated binding of Arfaptin to Rac1 regulates membrane ruffles (Tarricone *et al*., 2001) and that the BAR-like domain-containing proteins, such as FBP17, promotes invagination from the plasma membrane, which is regulated in an actin polymerization-dependent manner (Habermann, 2004; Itoh *et al*., 2005). In contrast, it has not been extensively studied that actin polymerization is required for the fission from endosomes, suggesting the possibility that tubulation and fission at the endosomes might be independent of Rac1-triggered actin reorganization. In cells depleted of SNX5 or DOCK180, the internalization of CD8-CI-MPR from the cell surface membrane was not affected, whereas its transport to TGN was impaired (Figure 5), suggesting that the SNX5-DOCK180 complex functions in the endosome-to-TGN trafficking. Importantly, however, this model does not necessarily exclude the role of DOCK180-induced Rac1 activation in the plasma membrane-to-early-endosome transport of CI-MPR and other cargos. In fact, the effect of DOCK180 deficiency on Rac1 activation is likely to be compensated by the other DOCK-family proteins, all of which activate Rac1 and/or Cdc42. In clear contrast, only DOCK180 binds to SNX5 (Supplemental

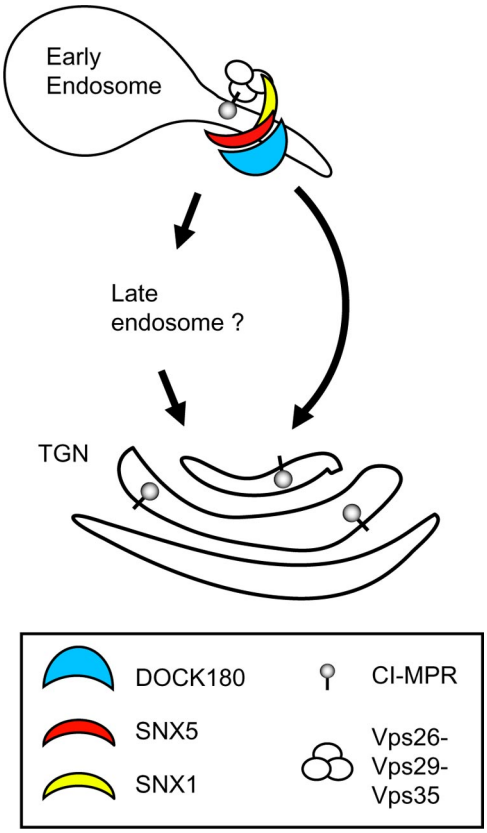

Figure 8. Summary diagram showing the participation of DOCK180 in retrograde transport of CI-MPR. DOCK180 (blue) directly interacts with SNX5 (red). SNX5 forms hetero-oligomer with SNX1 (yellow), which is a component of retromer complex and induces tubule formation from endosome through BAR domain. SNX5-DOCK180 complex may participate in this process by binding to SNX1. Another component of retromer complex, Vps26–Vps29–Vps35 subcomplex, functions as a cargo selection unit, and binds to CI-MPR (light gray). DOCK180 may recruit the retromer complex to late endosomes or TGN by interaction with phosphoinositides.

Figure S1B). This specificity may be the reason why we could observe the effect of DOCK180 deficiency only in the early-endosome-to-TGN transport.

In summary, we found that DOCK180 regulates transport of CI-MPR via SNX5 binding. In addition to CI-MPR, a wide range of cargo molecules are transported by the retromer-mediated retrograde machinery, e.g., sortilin and many bacterial exotoxins such as Shiga and cholera toxins (Seaman, 2004; Bujny *et al*., 2007). Although delivery of these toxins is governed basically by the retromer complex, the degree of SNX dependency varies among the toxins (Bujny *et al*., 2007). Therefore, examination of the fate of these cargos in SNX5- or DOCK180-deficient cells would further dissect the role of the SNX5-DOCK180 complex in the early-endosome-to-TGN retrograde transport.

ACKNOWLEDGMENTS

We thank Matthew N.J. Seaman for the generous gift of HeLaM cells, Jean-François Côté (Institut de Recherches, Cliniques de Montréal, Canada) for information on lipid-coated beads, Kazusa DNA Research Institute for providing cDNAs of the DOCK family, and Natsuko Yoshida, Noriko Fujimoto, Akiko Nishiyama, Keisho Fukuhara, and Yasuko Kasakawa for technical assistance. We also thank the staff of the Matsuda laboratory for technical advice and helpful input. This work was supported by grant-in-aid for scientific research on priority areas and the grant-in-aid of special coordination funds for promoting science and technology from the Ministry of Education, Culture, Sports and Science.

REFERENCES

Akagi, T., Sasai, K., and Hanafusa, H. (2003). Refractory nature of normal human diploid fibroblasts with respect to oncogene-mediated transformation. Proc. Natl. Acad. Sci. USA *100*, 13567–13572.

Aoki, K., Nakamura, T., Inoue, T., Meyer, T., and Matsuda, M. (2007). An essential role for the SHIP2-dependent negative feedback loop in neuritogenesis of nerve growth factor-stimulated PC12 cells. J. Cell Biol. *177*, 817–827.

Bujny, M. V., Popoff, V., Johannes, L., and Cullen, P. J. (2007). The retromer component sorting nexin-1 is required for efficient retrograde transport of Shiga toxin from early endosome to the trans Golgi network. J. Cell Sci. *120*, 2010–2021.

Carlton, J., Bujny, M., Peter, B. J., Oorschot, V. M., Rutherford, A., Mellor, H., Klumperman, J., McMahon, H. T., and Cullen, P. J. (2004). Sorting nexin-1 mediates tubular endosome-to-TGN transport through coincidence sensing of high-curvature membranes and 3-phosphoinositides. Curr. Biol. *14*, 1791–1800.

Carlton, J. G., Bujny, M. V., Peter, B. J., Oorschot, V. M., Rutherford, A., Arkell, R. S., Klumperman, J., McMahon, H. T., and Cullen, P. J. (2005). Sorting nexin-2 is associated with tubular elements of the early endosome, but is not essential for retromer-mediated endosome-to-TGN transport. J. Cell Sci. *118*, 4527–4539.

Cote, J. F., Motoyama, A. B., Bush, J. A., and Vuori, K. (2005). A novel and evolutionarily conserved PtdIns(3,4,5)P(3)-binding domain is necessary for DOCK180 signalling. Nat. Cell Biol. *7*, 797–807.

Cote, J. F. and Vuori, K. (2002). Identification of an evolutionarily conserved superfamily of DOCK180-related proteins with guanine nucleotide exchange activity. J. Cell Sci. *115*, 4901–4913.

Cozier, G. E., Carlton, J., McGregor, A. H., Gleeson, P. A., Teasdale, R. D., Mellor, H., and Cullen, P. J. (2002). The phox homology (PX) domain-dependent, 3-phosphoinositide-mediated association of sorting nexin-1 with an early sorting endosomal compartment is required for its ability to regulate epidermal growth factor receptor degradation. J. Biol. Chem. *277*, 48730–48736.

Di Paolo, G., and De Camilli, P. (2006). Phosphoinositides in cell regulation and membrane dynamics. Nature *443*, 651–657.

Erickson, M. R., Galletta, B. J., and Abmayr, S. M. (1997). *Drosophila* myoblast city encodes a conserved protein that is essential for myoblast fusion, dorsal closure, and cytoskeletal organization. J. Cell Biol. *138*, 589–603.

Fujioka, A., Terai, K., Itoh, R. E., Aoki, K., Nakamura, T., Kuroda, S., Nishida, E., and Matsuda, M. (2006). Dynamics of the Ras/ERK MAPK cascade as monitored by fluorescent probes. J. Biol. Chem. *281*, 8917–8926.

Fukui, Y. *et al*. (2001). Haematopoietic cell-specific CDM family protein DOCK2 is essential for lymphocyte migration. Nature *412*, 826–831.

Ganley, I. G., Espinosa, E., and Pfeffer, S. R. (2008). A syntaxin 10-SNARE complex distinguishes two distinct transport routes from endosomes to the trans-Golgi in human cells. J. Cell Biol. *180*, 159–172.

Gullapalli, A., Garrett, T. A., Paing, M. M., Griffin, C. T., Yang, Y., and Trejo, J. (2004). A role for sorting nexin 2 in epidermal growth factor receptor down-regulation: evidence for distinct functions of sorting nexin 1 and 2 in protein trafficking. Mol. Biol. Cell *15*, 2143–2155.

Gumienny, T. L. *et al*. (2001). CED-12/ELMO, a novel member of the CrkII/Dock180/Rac pathway, is required for phagocytosis and cell migration. Cell *107*, 27–41.

Habermann, B. (2004). The BAR-domain family of proteins: a case of bending and binding? EMBO Rep. *5*, 250–255.

Hasegawa, H., Kiyokawa, E., Tanaka, S., Nagashima, K., Gotoh, N., Shibuya, M., Kurata, T., and Matsuda, M. (1996). DOCK180, a major CRK-binding protein, alters cell morphology upon translocation to the cell membrane. Mol. Cell. Biol. *16*, 1770–1776.

Horazdovsky, B. F., Davies, B. A., Seaman, M. N., McLaughlin, S. A., Yoon, S., and Emr, S. D. (1997). A sorting nexin-1 homologue, Vps5p, forms a complex with Vps17p and is required for recycling the vacuolar protein-sorting receptor. Mol. Biol. Cell *8*, 1529–1541.

Itoh, T., Erdmann, K. S., Roux, A., Habermann, B., Werner, H., and De Camilli, P. (2005). Dynamin and the actin cytoskeleton cooperatively regulate plasma membrane invagination by BAR and F-BAR proteins. Dev. Cell *9*, 791–804.

Katoh, H. and Negishi, M. (2003). RhoG activates Rac1 by direct interaction with the Dock180-binding protein Elmo. Nature *424*, 461–464.

Kerr, M. C., Bennetts, J. S., Simpson, F., Thomas, E. C., Flegg, C., Gleeson, P. A., Wicking, C., and Teasdale, R. D. (2005). A novel mammalian retromer component, Vps26B. Traffic. *6*, 991–1001.

Kerr, M. C., Lindsay, M. R., Luetterforst, R., Hamilton, N., Simpson, F., Parton, R. G., Gleeson, P. A., and Teasdale, R. D. (2006). Visualisation of macropinosome maturation by the recruitment of sorting nexins. J. Cell Sci. *119*, 3967–3980.

Kiyokawa, E., Hashimoto, Y., Kobayashi, S., Sugimura, H., Kurata, T., and Matsuda, M. (1998a). Activation of Rac1 by a Crk SH3-binding protein, DOCK180. Genes Dev. *12*, 3331–3336.

Kiyokawa, E., Hashimoto, Y., Kurata, T., Sugimura, H., and Matsuda, M. (1998b). Evidence that DOCK180 up-regulates signals from the CrkII-p130^{Cas} complex. J. Biol. Chem. *273*, 24479–24484.

Kobayashi, S., Shirai, T., Kiyokawa, E., Mochizuki, N., Matsuda, M., and Fukui, Y. (2001). Membrane recruitment of DOCK180 by binding to PtdIns(3,4,5)P_3. Biochem. J. *354*, 73–78.

Kornfeld, S., and Mellman, I. (1989). The biogenesis of lysosomes. Annu. Rev. Cell Biol. *5*, 483–525.

Kurten, R. C., Cadena, D. L., and Gill, G. N. (1996). Enhanced degradation of EGF receptors by a sorting nexin, SNX1. Science *272*, 1008–1010.

Lamaze, C., Chuang, T. H., Terlecky, L. J., Bokoch, G. M., and Schmid, S. L. (1996). Regulation of receptor-mediated endocytosis by Rho and Rac. Nature *382*, 177–179.

Liu, H., Liu, Z. Q., Chen, C. X., Magill, S., Jiang, Y., and Liu, Y. J. (2006). Inhibitory regulation of EGF receptor degradation by sorting nexin 5. Biochem. Biophys. Res. Commun. *342*, 537–546.

Meller, N., Irani-Tehrani, M., Kiosses, W. B., Del Pozo, M. A., and Schwartz, M. A. (2002). Zizimin1, a novel Cdc42 activator, reveals a new GEF domain for Rho proteins. Nat. Cell Biol. *4*, 639–647.

Merino-Trigo, A., Kerr, M. C., Houghton, F., Lindberg, A., Mitchell, C., Teasdale, R. D., and Gleeson, P. A. (2004). Sorting nexin 5 is localized to a subdomain of the early endosomes and is recruited to the plasma membrane following EGF stimulation. J. Cell Sci. *117*, 6413–6424.

Natsume, T., Yamauchi, Y., Nakayama, H., Shinkawa, T., Yanagida, M., Takahashi, N., and Isobe, T. (2002). A direct nanoflow liquid chromatography-tandem mass spectrometry system for interaction proteomics. Anal. Chem. *74*, 4725–4733.

Nishihara, H., Kobayashi, S., Hashimoto, Y., Ohba, F., Mochizuki, N., Kurata, T., Nagashima, K., and Matsuda, M. (1999). Non-adherent cell-specific expression of DOCK2, a member of the human CDM-family proteins. Biochim. Biophys. Acta *1452*, 179–187.

Omi N *et al*. (2008). Mutation of Dock5, a member of the guanine exchange factor Dock180 superfamily, in the rupture of lens cataract mouse. Exp. Eye Res. *86*, 828–834.

Parks, W. T. *et al*. (2001). Sorting nexin 6, a novel SNX, interacts with the transforming growth factor-beta family of receptor serine-threonine kinases. J. Biol. Chem. *276*, 19332–19339.

Peter, B. J., Kent, H. M., Mills, I. G., Vallis, Y., Butler, P. J., Evans, P. R., and McMahon, H. T. (2004). BAR domains as sensors of membrane curvature: the amphiphysin BAR structure. Science *303*, 495–499.

Seaman, M. N. (2004). Cargo-selective endosomal sorting for retrieval to the Golgi requires retromer. J. Cell Biol. *165*, 111–122.

Seaman, M. N. (2005). Recycle your receptors with retromer. Trends Cell Biol. *15*, 68–75.

Seaman, M. N., McCaffery, J. M., and Emr, S. D. (1998). A membrane coat complex essential for endosome-to-Golgi retrograde transport in yeast. J. Cell Biol. *142*, 665–681.

Tarricone, C., Xiao, B., Justin, N., Walker, P. A., Rittinger, K., Gamblin, S. J., and Smerdon, S. J. (2001). The structural basis of Arfaptin-mediated cross-talk between Rac and Arf signalling pathways. Nature *411*, 215–219.

Teasdale, R. D., Loci, D., Houghton, F., Karlsson, L., and Gleeson, P. A. (2001). A large family of endosome-localized proteins related to sorting nexin 1. Biochem. J. *358*, 7–16.

Terai, K. and Matsuda, M. (2006). The amino-terminal B-Raf-specific region mediates calcium-dependent homo- and hetero-dimerization of Raf. EMBO J. *25*, 3556–3564.

Wassmer, T., Attar, N., Bujny, M. V., Oakley, J., Traer, C. J., and Cullen, P. J. (2007). A loss-of-function screen reveals SNX5 and SNX6 as potential components of the mammalian retromer. J. Cell Sci. *120*, 45–54.

Watabe-Uchida, M., John, K. A., Janas, J. A., Newey, S. E., and Van Aelst, L. (2006). The Rac activator DOCK7 regulates neuronal polarity through local phosphorylation of stathmin/Op18. Neuron *51*, 727–739.

Worby, C. A., and Dixon, J. E. (2002). Sorting out the cellular functions of sorting nexins. Nat. Rev. Mol. Cell Biol. *3*, 919–931.

Wu, Y. C., and Horvitz, H. R. (1998). *C. elegans* phagocytosis and cell-migration protein CED-5 is similar to human DOCK180. Nature *392*, 501–504.

Yajnik, V. *et al*. (2003). DOCK4, a GTPase activator, is disrupted during tumorigenesis. Cell *112*, 673–684.